Exact medial axis of quadratic NURBS curves

George M. Tzoumas*

Abstract

We study the problem of the exact computation of the medial axis of planar shapes the boundary of which is defined by piecewise conic arcs. The algorithm used is a tracing algorithm, similar to existing numeric algorithms. We trace the medial axis edge by edge. Instead of keeping track of points on the medial axis, we are keeping track of the corresponding footpoints on the boundary curves, thus dealing with bisector curves in parametric space. We exploit some algebraic and geometric properties of the bisector curves that allow for efficient trimming and we represent bifurcation points via their associated footpoints on the boundary, as algebraic numbers. The algorithm computes the correct topology of the medial axis identifying bifurcation points of arbitrary degree.

1 Introduction

The *medial axis* (MA) of an object can be defined as the locus of the centres of maximal bitangent disks and was originally introduced by [1]. The medial axis of a simple closed shape has a tree-like structure that provides an efficient shape representation. Along with a radius function, the MA allows for restoration of the original object, an operation called *medial axis transform* (MAT).

Due to its wide range of applications in biology, path planning and pattern analysis it has been studied extensively [4, 3, 11]. However most efforts consist of numerical algorithms to trace the bisector curves. Another approach is to approximate the boundary of the shape with simpler curves or line segments. However the resulting MA may require expensive post-processing, or be incorrect, as it is very sensitive to perturbations of the boundary of the shape.

Recently, with the availability of algebraic libraries and faster CPUs, there has been interest in exact algorithms following the exact computation paradigm. Successful examples of this approach are the exact and efficient arrangement of conic arcs and the Voronoi diagrams of circles and ellipses [7].

Following this trend, we apply exact computation techniques to the problem of medial axis computation. In theory, one can study some algebraic system and map the problem to the study of an arrangement of algebraic curves, parts of which are the medial axis

edges. However, this can lead to highly inefficient computations due to the degree and bitsize explosion of the computed quantities. Therefore, we focus on the parametric representation of the shape, trying to understand the deeper relation between simple geometric constructions (like the tangent line and the circle of curvature) and the parametric bisector curves.

We chose to use a simple $O(N^2)$ algorithm that also works with objects with holes. The algorithm includes a tracing step which we substitute with an exact one. Therefore, no tracing is included and all critical points are guaranteed to be identified. The idea is to start tracing the medial axis, always computing the next branching or terminal point in one step. The algorithm used is adapted from [12]. The branching point is the center of a maximal disk that is tangent to at least three distinct footpoints, while a terminal point corresponds to a local curvarture maximum ([4]). We work in the parametric space, in a manner similar to [13], however for efficient trimming of the bisector curves we exploit some algebraic and geometric properties.

2 Representation

The input is a simply connected closed shape consisting of a sequence of NURBS curves of degree 2, that is, conic arcs. The shape may contain holes, that are also piecewise conic arcs themselves. We follow the notation of [10]. The reason we focus on degree 2 NURBS curves is that they are powerful enough to express a wide variety of curves (elliptic, circular, hyperbolic, parabolic arcs) while keeping the algebraic complexity within reasonable bounds at the same time (comparison of algebraic numbers of degree 184 in the worst case). Given three control points $\mathbf{P_0}$, $\mathbf{P_1}$, $\mathbf{P_2}$ and a shape factor s (cf. Fig. 1), we represent a conic arc, parametrized by t, from $\mathbf{P_0}$ to $\mathbf{P_2}$ through $\mathbf{P_1}$ as

$$\mathbf{C}(t) = \frac{(1-t)^2\mathbf{P_0} + 2t(1-t)\frac{s}{1-s}\mathbf{P_1} + t^2\mathbf{P_2}}{(1-t)^2 + 2t(1-t)\frac{s}{1-s} + t^2}, \ t \in [0,1].$$

As parameter t traces the arc, we assume that the interior of the shape lies always on the left. Therefore, convex boundary arcs have positive or CCW orientation, while concave boundary curves have negative or CW orientation. The control points have the property that the segments $\mathbf{P_0P_1}$ and $\mathbf{P_1P_2}$ are tangent to $\mathbf{P_0}$ and $\mathbf{P_2}$ respectively. Note that $\mathbf{C}(0) = \mathbf{P_0}$ and $\mathbf{C}(1) = \mathbf{P_2}$. When $s < 1/2$ we have an ellipse, when

---

*INRIA Nancy Grand-Est

$s = 1/2$ we have a parabola, and $1/2 < s < 1$ yields a hyperbola, as shown in Fig. 1.
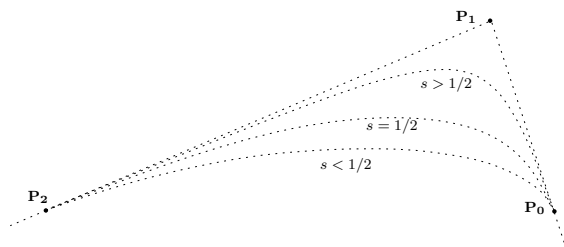

Figure 1: Definition of a quadratic NURBS arc.

3 Bisector curves

Each point on the medial axis is the center of a disk tangent to at least two points of the boundary of the shape. Therefore, the points of the medial axis lie on bisector curves of planar rational curves, or on bisector curves of a point and a curve. They may also lie on the self-bisector of a single curve. The bisector curve of planar rational curves is an algebraic curve and can be defined implicitly in the parametric space as the common intersection of the normal lines at the footpoints and the segment bisector of the footpoints themselves [5]. It is of lower degree than the implicit equation in the cartesian space. We can verify that for conics, the bisector equation in the parametric space is of total degree 12 in the worst case, 6 in each parameter. See [6] for the case of ellipses and [9, 5] for a study of point-curve or curve-curve bisectors. We represent a point on the medial axis by the corresponding footpoints on the boundary curves, therefore we can represent parts of the medial axis by properly trimming the bisector curves. In [13] the bisector curves are split in monotone pieces by using a subdivision technique. In the section that follows we improve this technique by proving and exploiting some algebraic and geometric properties of the bisector curves themselves. This is a generalization of the properties observed and exploited in [6].

4 Maximal bitangent disk

The boundary of the shape consists of two types of arcs. Convex and concave ones. We consider the general case where the tangency points of a maximal bitangent disk are not a concave joint. Let a_1 and a_2 be two arcs and $\mathbf{P_1}$ and $\mathbf{P_2}$ the corresponding footpoints of a maximal bitangent disk B (Fig. 2). Given $\mathbf{P_1}$, since the bisector curve is of degree 6 in each parameter, there may be up to 6 candidate points for $\mathbf{P_2}$. We can select the proper solution by applying the following lemmas.

Lemma 1 *If a_1 is concave, then the tangent line T*

of a_1 at $\mathbf{P_1}$ separates $\mathbf{P_2}$ and a_1 (Fig. 2 cases (i) and (ii)). If a_1 is convex, then the circle of curvature of a_1 at $\mathbf{P_1}$ contains $\mathbf{P_2}$ (Fig. 2 cases (iii) and (iv)).

Proof. If a_1 is concave, then a_1 and the maximal disk B have opposite curvatures. Therefore all points of a_1 (except $\mathbf{P_1}$) and B are separated by T. (In this case, T can be seen as a circle with an infinite radius.) If a_1 is convex, then the circle of curvature of a_1 at $\mathbf{P_1}$ is the circle of maximum radius that lies locally inside a_1. Therefore its radius bounds from above the radius of B. □

Applying the above lemma for $\mathbf{P_2}$ yields the following.

Lemma 2 *If a_2 is concave (Fig. 2 cases (i) and (iii)), we consider the tangent lines of a_2 along the arc. At some point $\mathbf{Q}$, the tangent line may pass through $\mathbf{P_1}$ and this will be a boundary condition, that is before $\mathbf{Q}$, $\mathbf{P_1}$ will be on the correct side (left) of the tangent line, while after $\mathbf{Q}$, $\mathbf{P_1}$ will be on the right of the tangent line, thus points after $\mathbf{Q}$ on a_2 are rejected. If a_2 is convex (Fig. 2 cases (ii) and (iv)), we consider the cirles of curvature of a_2 along the arc. At some point $\mathbf{Q}$, the circle of curvature may pass through $\mathbf{P_1}$ and this will be a boundary condition, that is before $\mathbf{Q}$, $\mathbf{P_1}$ will be inside the circle of curvature, while after $\mathbf{Q}$, $\mathbf{P_1}$ will be outside the circle of curvature, therefore points after $\mathbf{Q}$ on a_2 are rejected.*

Algebraically, the tangent line of a_1 evaluated at a point of a_2 is a bivariate polynomial of total degree 4, 2 in each parameter. The circle of curvature of a_1, evaluated at a point of a_2 is a bivariate polynomial of total degree 10, 6 in t_1 and 4 in t_2. Fig. 3 (i) shows an instance of Fig. 2, case (iii), where a_1 is a convex arc and a_2 is a concave one. The graph of Fig. 3 (ii) shows a plot of the parametric bisector (solid line graph). The dashed line graph is a plot of the circle of curvature of a_1 evaluated at a point of a_2. Note that the bisector critical points are separated by the graph of the circle of curvature, providing automatically a subdivision in monotone pieces. This is because at those critical points, the circle of curvature is also a maximal bitangent disk. Similar properties hold for all cases of Fig. 2. Location of the bisector extrema via the circle of curvature is more efficient, because purely algebraic techniques study the bisector curve itself via a discriminant, which has some spurious factors [2]. The reason is that the bisector is not an arbitrary curve but it is computed as some resultant of an algebraic system [5, 6, 7].

5 Critical points

Three-prong points (Fig. 4). A three-prong point on the medial axis is a point where the associated maximal disk is tangent to three points of the boundary of
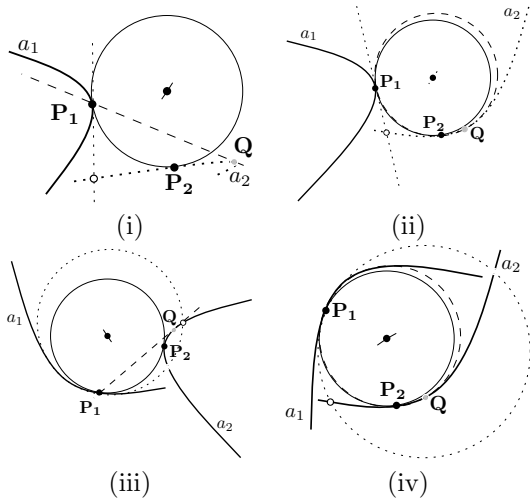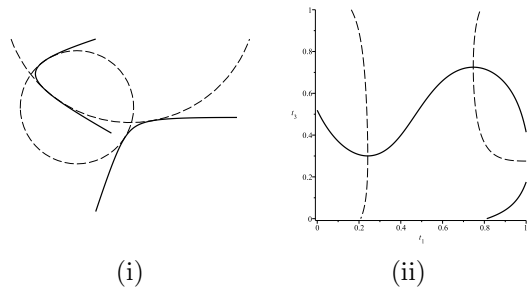
Figure 2: Isolating the proper footpoint.

Figure 3: (i) A convex and a concave arc with the circles of curvature corresponding to parametric bisector extrema. (ii) Parametric bisector and circle of curvature evaluated.

the shape. The points of tangency can be described by an algebraic system. The system can be formulated and solved in a way similar to [7].

Terminal points. They are associated with the circle of curvature at points where the curvature attains a local maximum. These can be considered as degenerate cases of (iii), (iv) and (v) in Fig. 4.

Arc joints. These points are in fact artifacts, due to the fact that a single curve is considered as two or more subcurves. Thus, combinatorially, one has to take into account the MA points corresponding to the arc joints.

Let a_1, a_2, a_3 be three conic arcs on the boundary of the shape, with parameters t_1, t_2, t_3 respectively. We express a tritangent circle to a_1, a_2, a_3 by an algebraic system. Footpoint parameter value t_1 can be expressed as a resultant polynomial the degree of which is shown in table 1. The most difficult case is for three conic arcs, where the degree of the polynomial is 184, as in the case for the Voronoi diagram of ellipses [6]. Table 1 also summarizes the simpler cases, when the second footpoint lies on the same arc, or when one footpoint corresponds to an arc endpoint and there-

fore it is a fixed rational point. The equations used to describe each algebraic system are i) the normal lines N_i at the footpoint of arc a_i, ii) the segment bisector M_{ij} which is perpendicular to the segment joining the footpoints of a_i (or endpoint p_i) and a_j (or p_j), iii) the bisector curve B_{ij} of arcs a_i and a_j or the self-bisector curve B_{ii} of arc a_i.

Computing the footpoint as an algebraic number allows for detection of n-prong points, that is bifurcation points of degree ≥ 3, simply by comparing such algebraic numbers. For example, if there exist a maximal disk tangent to a_1, a_2, a_3, a_4 then the footpoints of the tritangent disks of a_1, a_2, a_3 and a_1, a_2, a_4 on arc a_1 are identical.

Finally, the solution of the algebraic systems of table 1 can be accelerated by incorporating the subdivision technique of [8], because after applying lemmas 1 and 2, the bisectors are split in monotone parts.

	t_2	t_3	deg.	equations				
(i)	a_2	a_3	184	N_1	N_2	N_3	M_{12}	M_{13}
(ii)	p_2	a_3	36	N_1	N_3	M_{12}	M_{23}	
(iii)	a_1	a_2	32	N_1	N_2	M_{12}	B_{11}	
(iv)	a_2	a_2	16	N_1	N_2	M_{12}	M_{22}	B_{22}
(v)	a_1	p_2	8	B_{12}	B_{22}			
(vi)	p_2	p_3	6	N_1	M_{12}	M_{13}		

Table 1: Degree of footpoints for 3-prong MA points (Fig. 4.)

6 Computing the medial axis

The MA is constructed in a way similar to [12]. Instead of tracing the MA via the boundary of the shape with a predefined precision, we check explicitly each critical point, expressed with an algebraic system, as discussed in the previous section. Thus, we trace the MA in a constant number of steps, depending only on the number of input arcs (and not on some precision threshold).

We conclude with an example applying the above techniques. Consider the 9 control points $\mathbf{P_0} \ldots \mathbf{P_7}, \mathbf{P_8} \equiv \mathbf{P_0}$ with coordinates $(1, 5)$, $(-5, 3)$, $(2, -1)$, $(0, -1)$, $(1, -6)$, $(3, 0)$, $(10, 0)$, $(3, 3)$, $(1, 5)$ defining 4 arcs with shape factors 2/3, 1/4, 4/5, 3/5 respectively, where arc a_{i+1} has control points $(\mathbf{P_{2i}}, \mathbf{P_{2i+1}}, \mathbf{P_{2i+2}})$, $i = 0 \ldots 3$, as shown in Fig. 5. We may start from a convex vertex (i.e., $\mathbf{P_8}$) and trace the boundary of the shape, checking for critical points of the medial axis. This way the medial axis is traced edge by edge. Note that there exist two tritangent disks of a_1, a_3, a_4. However, the dashed one is rejected, as its associated footpoint on a_4 lies after the footpoint of the other tritangent disk, as we move from $\mathbf{P_8}$ to $\mathbf{P_0}$.
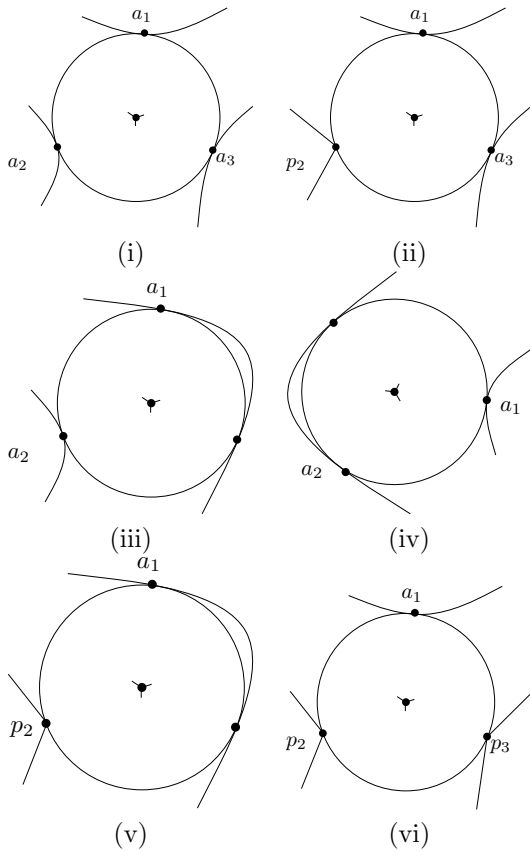
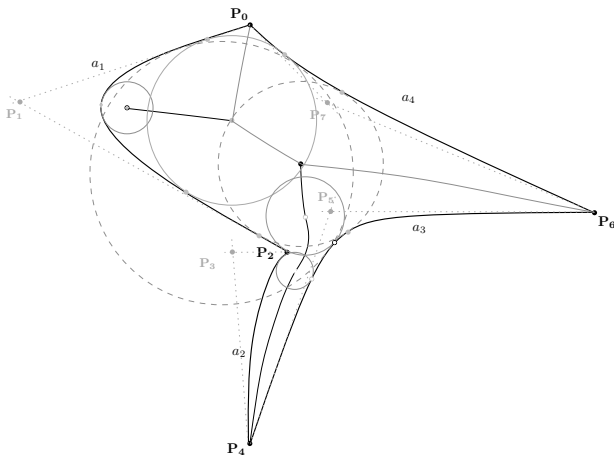Figure 4: Various types of three-prong points

Figure 5: Medial axis of a shape and the maximal disks at its critical points.

References

[1] Harry Blum. A Transformation for Extracting New Descriptors of Shape. In Weiant Wathen-Dunn, editor, *Models for the Perception of Speech and Visual Form*, pages 362–380. MIT Press, Cambridge, 1967.

[2] L. Busé and B. Mourrain. Explicit factors of some iterated resultants and discriminants. *Mathematics of Computations*, 78:345–386, 2009.

[3] Hyeong In Choi, Sung Woo Choi, and Hwan Pyo Moon. Mathematical theory of medial axis transform. *Pacific Journal of Mathematics*, 181(1):57–88, 1997.

[4] J. J. Chou. Voronoi diagrams for planar shapes. *IEEE Comput. Graph. Appl.*, 15(2):52–59, 1995.

[5] G. Elber and Myung-Soo Kim. Bisector curves of planar rational curves. *Comp.-Aid. Des.*, 30:1089–1096, 1998.

[6] I. Z. Emiris, E. P. Tsigaridas, and G. M. Tzoumas. Predicates for the exact Voronoi diagram of ellipses under the euclidean metric. *Intern. J. Comp. Geom. & Appl.*, 18(6):567–597, 2008.

[7] I.Z. Emiris, E.P. Tsigaridas, and G.M. Tzoumas. Exact Delaunay graph of smooth convex pseudocircles: general predicates, and implementation for ellipses. In *SPM '09: 2009 SIAM/ACM Joint Conf. on Geom. & Phys. Model.*, pages 211–222, San Francisco, CA, USA, 2009.

[8] I.Z. Emiris and G.M. Tzoumas. Exact and efficient evaluation of the InCircle predicate for parametric ellipses and smooth convex objects. *Comp.-Aid. Des.*, 40(6):691–700, 2008.

[9] R.T. Farouki and R. Ramamurthy. Degenerate point/curve and curve/curve bisectors arising in medial axis computations for planar domains with curved boundaries. *Computer Aided Geometric Design*, 15:615–635, 1998.

[10] Les Piegl and Wayne Tiller. *The NURBS book (2nd ed.)*. Springer-Verlag New York, Inc., New York, NY, USA, 1997.

[11] R. Ramamurthy and R. T. Farouki. Voronoi diagram and medial axis algorithm for planar domains with curved boundaries - II: Detailed algorithm description. *J. Comput. Appl. Math.*, 102(2):253–277, 1999.

[12] M. Ramanathan and B. Gurumoorthy. Constructing medial axis transform of planar domains with curved boundaries. *Comp.-Aid. Des.*, 35(7):619–632, 2003.

[13] J.-K. Seong, E. Cohen, and G. Elber. Voronoi diagram computations for planar NURBS curves. In *Proc. 2008 ACM Symp. Solid and Phys. Modeling*, pages 67–77, New York, NY, USA, 2008. ACM.